IMMUNOLOGY

Human gingival mesenchymal stem cells retain their growth and immunomodulatory characteristics independent of donor age

Jay R. Dave[1], Sayali S. Chandekar[1], Shubhanath Behera[2], Kaushik U. Desai[1], Pradnya M. Salve[1], Neha B. Sapkal[1], Suhas T. Mhaske[1], Ankush M. Dewle[1], Parag S. Pokare[1], Megha Page[3], Ajay Jog[3], Pankaj A. Chivte[4], Rupesh K. Srivastava[5], Geetanjali B. Tomar[1]*

Aging has been reported to deteriorate the quantity and quality of mesenchymal stem cells (MSCs), which affect their therapeutic use in regenerative medicine. A dearth of age-related stem cell research further restricts their clinical applications. The present study explores the possibility of using MSCs derived from human gingival tissues (GMSCs) for studying their ex vivo growth characteristics and differentiation potential with respect to donor age. GMSCs displayed decreased in vitro adipogenesis and in vitro and in vivo osteogenesis with age, but in vitro neurogenesis remained unaffected. An increased expression of p53 and SIRT1 with donor age was correlated to their ability of eliminating tumorigenic events through apoptosis or autophagy, respectively. Irrespective of donor age, GMSCs displayed effective immunoregulation and regenerative potential in a mouse model of LPS-induced acute lung injury. Thus, we suggest the potential of GMSCs for designing cell-based immunomodulatory therapeutic approaches and their further extrapolation for acute inflammatory conditions such as acute respiratory distress syndrome and COVID-19.

INTRODUCTION

Mesenchymal stem cell (MSC)–based tissue regenerative approaches have gained a lot of importance in the past decade due to their self-renewal and multilineage differentiation potentials, as well as immunomodulatory properties. The major advantage with MSCs is their prompt availability in clinically relevant quantities for therapeutic purposes in both acute and chronic diseases (*1*). Before treatment, MSCs can be expanded in vitro over several population doublings (*1*). However, extensive subculturing has been reported to result in fundamental loss of MSC morphology, migration and differentiation potentials, diminished cytoskeleton turnover, and compromised mitochondrial morphology, eventually increasing their susceptibility toward senescence (*1*–*3*). In addition to the in vitro replicative senescence, researchers have also been intrigued about whether MSCs from elderly individuals could provide the same healing effect as those of their young counterparts, from clinical and translational points of view. Results from systems-level analysis demonstrate the deleterious effects of natural aging on the quality and potency of MSCs, thus impeding the availability of a large number of MSCs for autologous transplantation (*1*, *4*–*9*). Moreover, limitations in terms of frequent sampling hamper the availability of allogeneic MSCs for multiple administrations (*1*, *9*).

Aging increases the risk of diseases and exacerbates damage caused by injury and trauma. A progressive decline in stem cell pool results in low MSC numbers and deteriorated function with age. The above statements are based on several previous reports that present the detrimental effects of aging on the quantity and quality of MSCs derived from bone marrow (BM), adipose tissue (AT), periodontal ligament (PDL), and dental pulp (DP) (*6*, *10*–*21*). As a result, a paucity of data related to explicit testing of aging MSCs in clinical trials forbids the designing of cell-based therapeutic approaches for the aged. As the elderly population is the primary target for cell-based therapies, it becomes essential to undertake reproducible strategies for supplementing sufficient numbers of clinically competent MSCs and assess them rigorously.

MSCs from gingival tissues have gained vast attention in the past decade due to the ease of tissue harvesting, abundant cell yield, and fast healing of the donor site (*22*–*27*). However, very few reports elaborate on their senescence and its effect on stem cell function. Therefore, with the goal of using gingival tissue–derived MSCs (GMSCs) for regenerative therapies such as bone regeneration and immunoregulation, we addressed some key questions: (i) Does donor age affect the in vitro growth and phenotypic characteristics of human GMSCs? (ii) What is the effect of aging on the functional properties of GMSCs, including their multilineage differentiation potential? (iii) Does donor age affect the in vitro and in vivo immunomodulatory and regenerative potential of GMSCs in an animal model of lipopolysaccharide (LPS)–induced acute lung injury? In light of these considerations, we studied the biological properties of GMSCs in relation to donor age. In contrast to several previous studies related to BM, AT, PDL, and DP, which report an age-associated decline in both quality and quantity of MSCs, our data depicted that the age of donor does not deter all the properties of GMSCs (*4*, *10*, *11*, *13*, *16*, *20*, *21*, *28*–*36*). A detailed analysis of in vitro cellular morphology, surface markers, proliferation capacity (colony formation and population doublings), aging markers [senescence-associated β-galactosidase (SA-β-gal), p53, and CDKN2A], and cellular migration showed that increased donor age does not deteriorate GMSCs in terms of their quantity and quality. Moreover, GMSCs exhibited a skewed differentiation toward neuronal lineage, which was unaffected by age, but a decline in adipogenic and osteogenic lineages was observed. In addition, we

[1]Institute of Bioinformatics and Biotechnology, Savitribai Phule Pune University, Pune, 411007 Maharashtra, India. [2]National Centre for Cell Science, Savitribai Phule Pune University Campus, Pune, 411007 Maharashtra, India. [3]Department of Dentistry, Deenanath Mangeshkar Hospital and Research Centre, Pune, 411004 Maharashtra, India. [4]Saraswati Danwantri Dental College and Hospital, Parbhani, 431401 Maharashtra, India. [5]Department of Biotechnology, All India Institute of Medical Science, New Delhi 110029, India.
*Corresponding author. Email: geetanjalitomar13@gmail.com

also observed that in vitro and in vivo immunosuppressive behavior of GMSCs in an LPS-induced acute lung injury (ALI) model was independent of donor age.

RESULTS

Growth and phenotypic characterization

In vitro growth and phenotypic characteristics of GMSCs are independent of donor age

To determine the effect of donor age on growth and phenotypic characteristics of in vitro GMSC population, we evaluated GMSCs from all the age groups for colony formation, proliferation, population doublings, and expression of MSC surface markers. GMSCs obtained from groups A, B, and C exhibited plastic adherent fibroblast morphology during primary culture, which was independent of donor age (passage 0) (Fig. 1, A and C to E). These cells were found to retain their fibroblast morphology even during long-term in vitro culture (passages 8 and 12) (Fig. 1, F to K). In terms of cell proliferation, a comparative analysis by 3-(4,5-Dimethylthiazol-2-yl)-2,5-Diphenyltetrazolium Bromide (MTT) assay suggested no substantial difference between GMSCs of different age groups (Fig. 1B). We observed that GMSCs from all the age groups efficiently formed colonies, although the colonies of group A GMSCs were larger in size (Fig. 1, L to N and Q). The colony formation efficiency indicates the clonal potential of stem cells. However, the population doubling time (PDT) for GMSCs of group C significantly increased at higher passage, but the doublings reduced between passages 9 and 13 (Fig. 1, O and P, respectively). The increase in PDT in group C GMSCs can be attributed to in vitro replicative senescence. The above results are in support of the previous reports that demonstrated that donor age does not decrease the in vitro proliferative behavior of dental stem cells during early passages *(14*, *16)*.

GMSCs between passages 2 and 10 were analyzed for expression of MSC surface markers by flow cytometry analysis. Our results

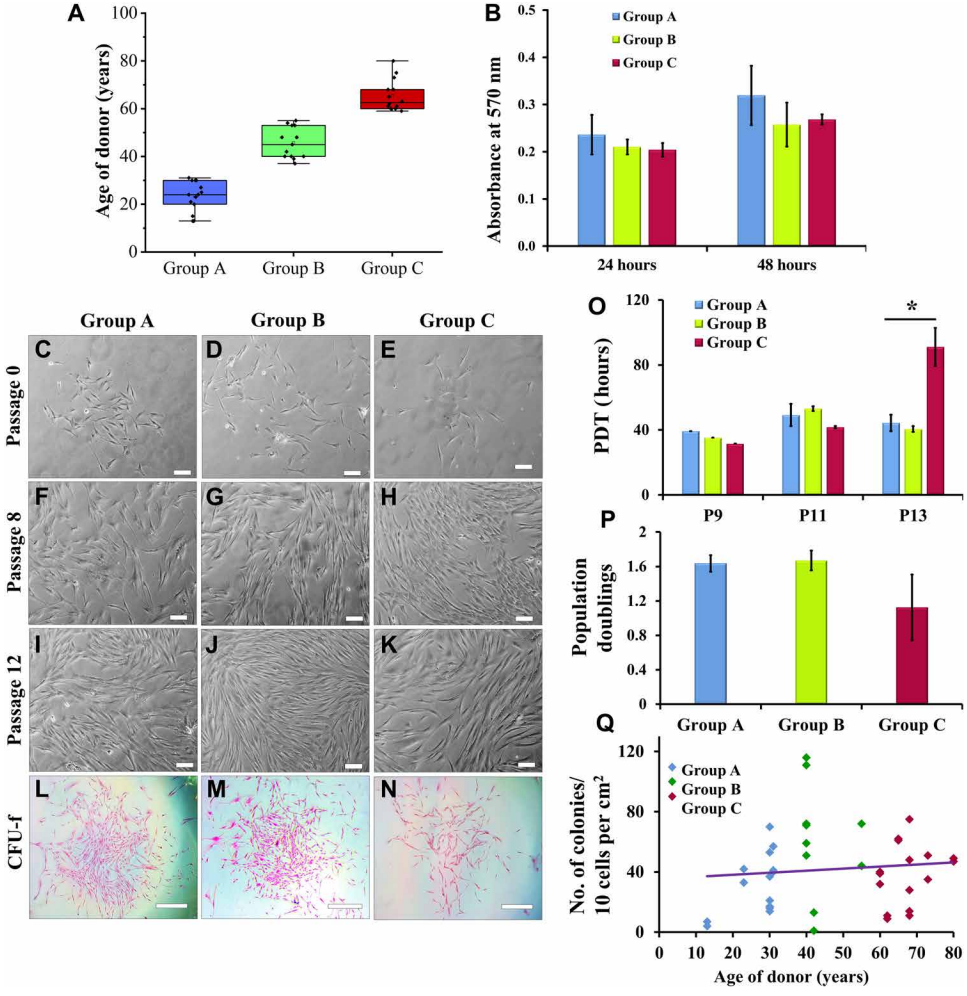

Fig. 1. In vitro morphological and growth characteristics of GMSCs. (**A**) Age distribution of donors categorized into group A (13 to 31 years; mean age ± SD, 23.29 ± 6.26 years; $n = 14$), group B (37 to 55 years; mean age ± SD, 45.69 ± 6.49 years; $n = 13$), and group C (59 to 80 years; mean age ± SD, 65.36 ± 6.57 years; $n = 14$). (**B**) GMSCs from all age groups displayed almost similar average rate of proliferation between passages 8 and 11. (**C** to **K**) GMSCs from groups A, B, and C displayed spindle-shaped fibroblast morphology in the in vitro cultures (magnification, ×10; scale bars, 100 μm) at passages 0, 8, and 12. (**L** to **N**) The size of colonies in group A GMSCs is larger than that in group C (eosin staining, pink) (magnification, x4; scale bars, 500 μm). (**O**) Group A, B, and C GMSCs displayed similar PDT at passages 9 and 11, but the doubling time of group C GMSCs significantly increased at passage 13. (**P**) No significant difference in average population doublings is observed between passages 9 and 13 (*$P < 0.05$, all pairwise multiple comparison). (**Q**) GMSCs from all the groups showed similar efficiency of colony formation.

reveal that 80 to 90% GMSCs from all the passages express MSC surface markers including CD44, CD90, CD73, and CD105, without any contamination of hematopoietic cells (negligible expression of CD34 and CD45), indicating that GMSCs from all age group of donors establish homogeneous culture in vitro (Fig. 2A). In addition, GMSCs exhibited a high expression of these surface markers, as quantified by the mean fluorescence intensity (MFI) (Fig. 2B). Our results are in consensus with the previous studies related to BM- and DP-derived MSCs, which suggest that cell surface marker expression is not indicative of the differentiation state of cells or their potency and is not able to distinguish between MSCs obtained from young and old donors (*4*, *9*, *34*).

GMSCs from young donors expand rapidly and undergo faster in vitro replicative senescence

The augmented lysosomal content of aged cells is represented by the activity of specific lysosomal SA-β-gal, which is studied as the most common biomarker for identification of senescent cells. In our experiments, we detected the presence of senescing cell population in early passage (indicative of in vivo cellular aging with respect to donor age) and late passage (indicative of in vitro replicative senescence) GMSC cultures by staining them for SA-β-gal. Figure 2 (C to E) represents the number of SA-β-gal^{+ve} cells in in vitro cultures of GMSCs between passages 8 and 12. GMSC cultures from group C displayed a significantly large number of SA-β-gal^{+ve} cells both in early (passages 4 to 6; average number of SA-β-gal^{+ve} cells = 136.25 ± 44.9) (Fig. 2F) and late passages (passages 9 to 12; average number of SA-β-gal^{+ve} cells = 279.5 ± 27.7) (Fig. 2G). Group A GMSCs exhibited rapid in vitro replicative senescence as compared to cultures from groups B and C. Group A GMSCs displayed a 13.5-fold increase in SA-β-gal^{+ve} cells in late passage as compared to early passage, whereas groups B and C showed 0.75- and 1.05-fold increase, respectively (Fig. 2, F and G). These findings support our previous observations with respect to the number of population doublings that the cells undergo during their life cycle. Every cell has a Hayflick's limit that defines the number of doublings it might undergo during its entire life before undergoing senescence-associated apoptosis (*37*, *38*). As GMSCs derived from adults and elderly population have already been subjected to a large number of doublings in vivo, their in vitro population doublings and the rate of in vitro aging decline. On the other hand, the younger GMSC cultures rapidly multiply to double their population in vitro and thus quickly progress toward in vitro replicative senescence (Fig. 2, F and G).

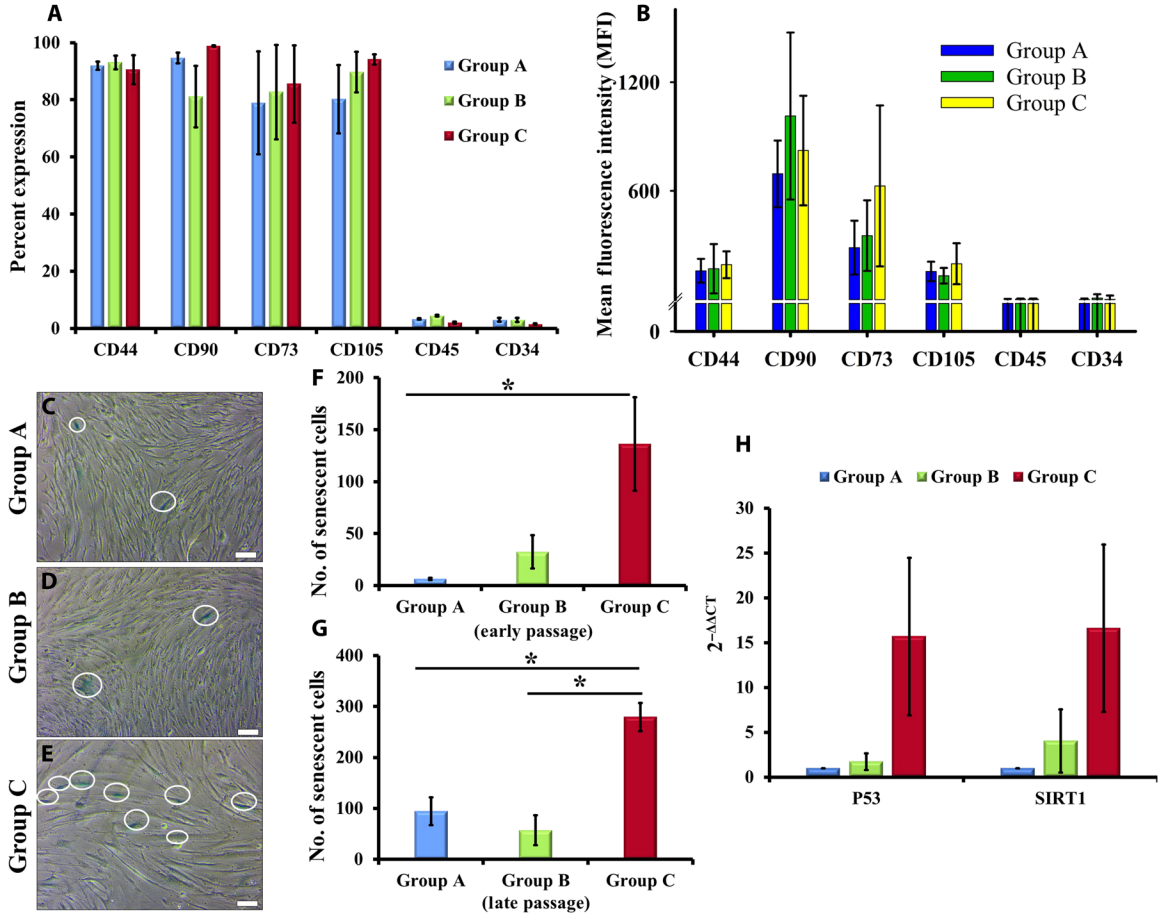

Fig. 2. Stem cell and senescence markers. (**A** and **B**) Group A, B, and C GMSCs expressed MSC surface markers (CD44, CD90, CD73, and CD105) with negligible expression of hematopoietic stem cell markers (CD45 and CD34). (**C** to **E**) Representative images of SA-β-gal^{+ve} cells (blue-green color of SA-β-gal–stained cells, highlighted in the figure; magnification, ×10; scale bars, 100 μm) between passages 8 and 12. (**F** and **G**) GMSCs from group C showed significantly higher population of senescing cells in both early (average of passages 4 to 6) and late passage (average of passages 9 to 12) (*$P < 0.05$, all pairwise multiple comparison). (**H**) Group C GMSCs displayed enhancement in the expression of p53 and SIRT1. The gene expression profiles of group B and C GMSCs were normalized with group A.

Senescence in terms of SA-β-gal expression is suggestive of an aging cell population, with apoptosis or autophagy as cell's ultimate fate. To support our speculation that, with increase in donor age, GMSCs eliminate possibilities of tumorigenic events and maintain a healthy stem cell pool (*37*, *38*), we detected an enhanced expression of p53 (15-fold) and sirtuin1 (SIRT1) (16-fold) in group C GMSCs as compared to group A (Fig. 2H). These findings suggest that to nullify the detrimental effects of aging on the tissue and eliminate the possibility of tumorigenic events, the inherent cell population undergoes either apoptosis (by up-regulation of p53 expression) or autophagy (elevated levels of SIRT1) to exclude senescent cells.

In continuation to the above findings, we further observed a high level of CDKN2A (p16) in group C GMSCs (Fig. 3A), which indicated an efficient DNA damage response under variable stress conditions, to prevent aging-associated tumorigenic events. CDKN1A (p21) did not display a notable change in GMSCs of groups A and C. Thus, we conclude that a high level of p53 in group C GMSCs is correlated to the maintenance of genomic integrity by suppressing pathological/dysplastic proliferation or aberrant differentiation in aging tissues. We also observed that this age-related depletion of cell population due to apoptosis or autophagy was compensated by an increase in expression of growth factor receptors such as PDGFR (platelet-derived growth factor receptor), FGFR (fibroblast growth factor receptor), and EGFR (epidermal growth factor receptor) by GMSCs (Fig. 3B). This result suggests that GMSCs enhance their proliferation to combat the increasing stress conditions with age to maintain tissue homeostasis. All these findings point toward the capability of GMSCs to combat the increasing stress conditions that build up in the periodontal tissue with age, thus eventually facilitating sustenance of proliferative expansion for maintenance of healthy stem cell pool in the gingival tissue.

Along with the maintenance of healthy stem cell population, migration to the site of damage in response to cytokines for the purpose of wound healing is also necessary for maintaining tissue homeostasis. However, cell migration may vary under in vitro and in vivo environmental conditions, thus affecting the process of tissue repair. In our in vitro cultures, we observed that GMSCs from group B displayed the highest rate of cell migration as compared to groups A and C (Fig. 3, C to L, and movie S1). As the difference was not very large, it still further strengthened our conclusion that, in contrast to several other sources of MSCs including BM, AT, PDL, and DP, the growth and phenotypic characteristics of GMSCs remained largely unaffected by the age of donor (*4*, *10*, *11*, *13*, *16*, *20*, *21*, *28*–*36*).

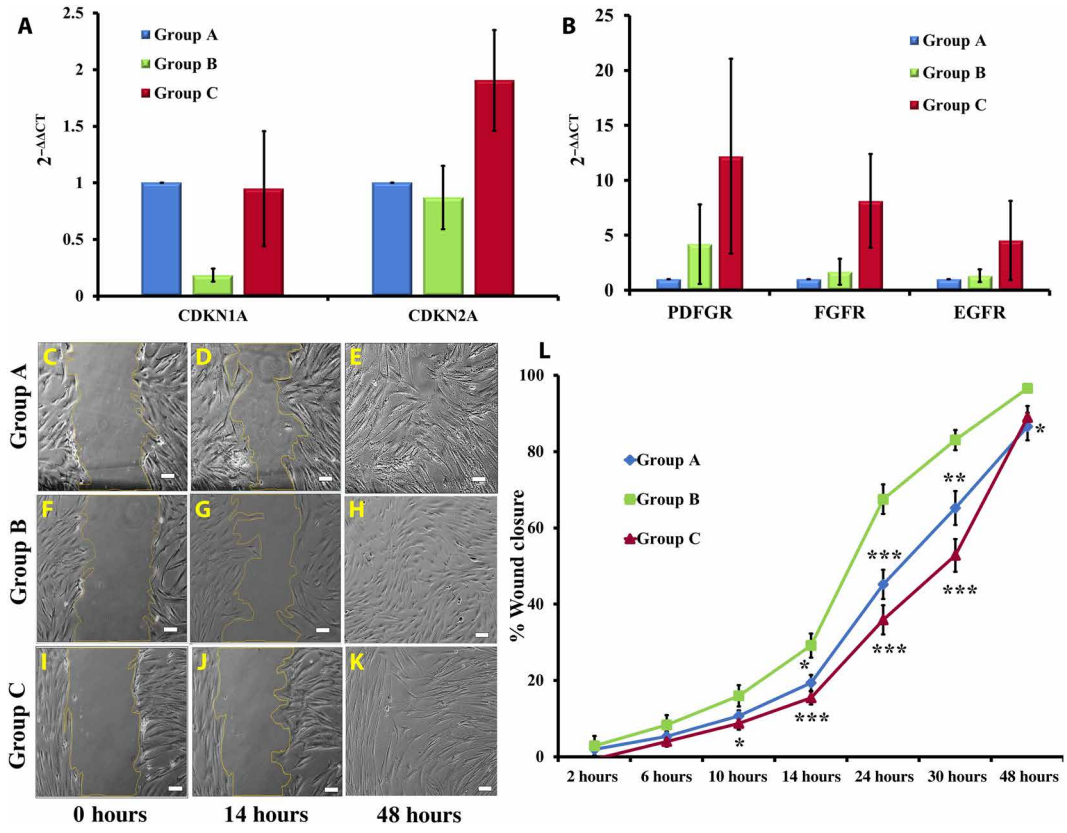

Fig. 3. Cell cycle regulators, growth factor receptors, and wound healing ability. (**A**) Group C GMSCs displayed an up-regulation in expression of CDKN2A as compared to groups A and B. No significant difference in levels of CDKN1A was observed. (**B**) As compared to groups A and B, group C GMSCs exhibited an increased expression of growth factor receptors (PDGFR, FGFR, and EGFR). The gene expression profiles of group B and C GMSCs were normalized with group A. (**C** to **L**) Group B GMSCs displayed a significantly higher rate of migration as compared to groups A and C. There was very low but consistent difference in the rate of wound closure in all groups of GMSCs (magnification, ×10; scale bars, 100 μm) (at time point 10 hours, for group B versus group C, $^{*}P < 0.05$; at time point 14 hours, for group A versus group B, $^{*}P < 0.05$ and for group B versus group C, $^{***}P < 0.001$; at time point 24 hours, for group A versus group B and group B versus group C, $^{***}P < 0.001$; at time point 30 hours, for group A versus group B, $^{**}P < 0.01$ and for group B versus group C, $^{***}P < 0.001$; at time point 48 hours, for group A versus group B, $^{*}P < 0.05$).

Functional characterization—Multilineage differentiation

Multilineage differentiation of GMSCs is skewed toward neurogenesis

To determine the effect of donor age on multilineage differentiation potential of GMSCs, we induced the cultures for adipogenic, osteogenic, and neurogenic differentiation. The GMSCs from group A displayed early signs of adipogenic differentiation and accumulated a large number of oil globules as compared to GMSCs of groups B and C. Moreover, the percentage of cells that differentiated into adipocytes was also significantly higher in group A GMSCs than in group C GMSCs (Fig. 4, A to D).

Osteogenesis in GMSCs was observed by the appearance of mineralized bone nodules at 14 to 16 days of differentiation (Fig. 4, E to G). Although no difference was observed in the levels of alkaline phosphatase (ALP) (Fig. 4H), the calcium phosphate mineralization stained using alizarin red S (ARS) (Fig. 4, I to K) showed a

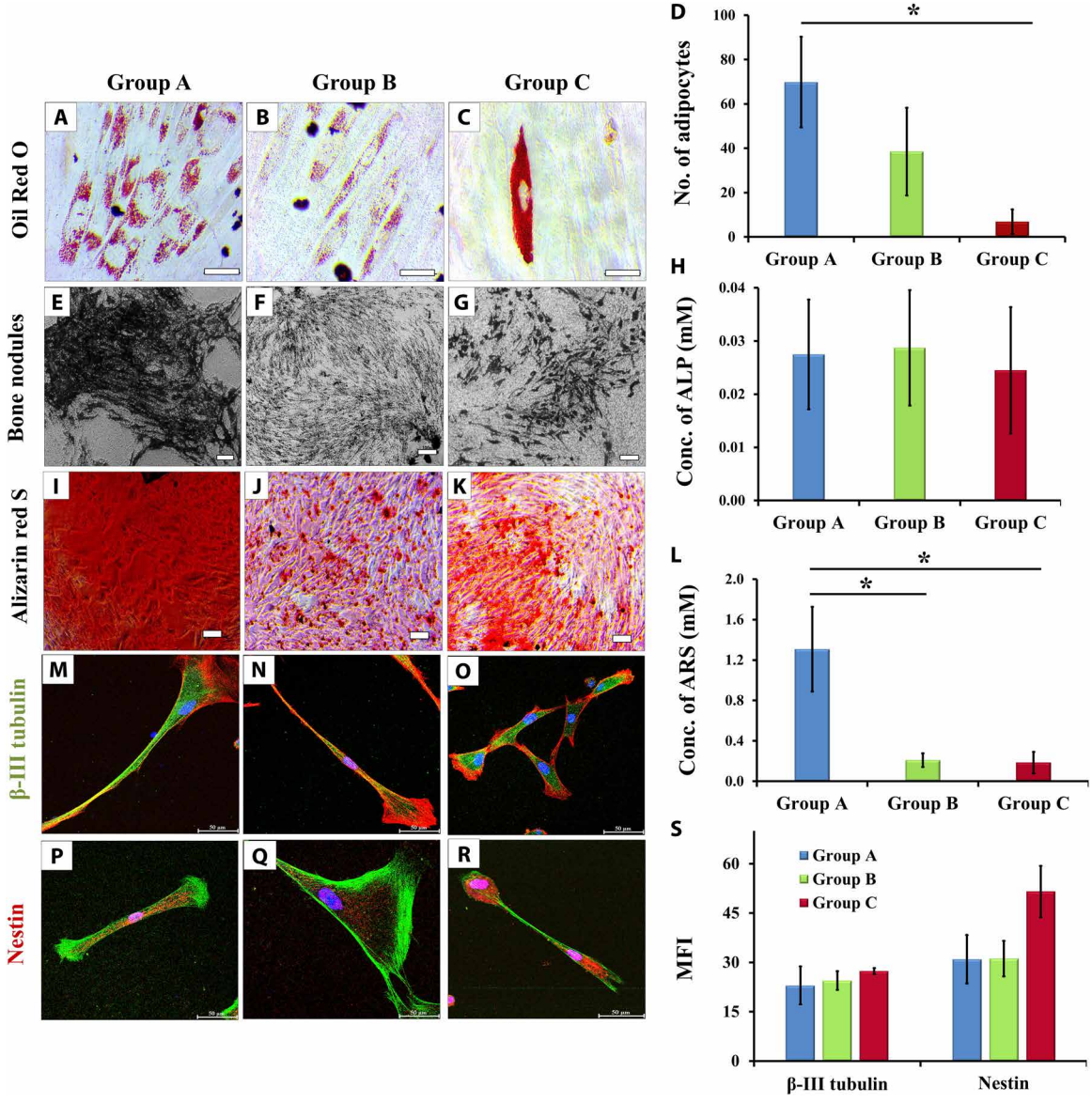

Fig. 4. Multilineage differentiation potentials. (**A** to **C**) Accumulation of oil globules by GMSCs of all groups (magnification, ×40; scale bars, 50 μm; oil globules accumulated inside the cells are stained with Oil Red O, which gives red color). (**D**) The number of oil globules declined with donor age (*$P < 0.05$, group A versus group C). (**E** to **G**) The osteogenic differentiation potential of GMSCs also showed a decline with donor age, in terms of decrease in bone nodule formation (magnification, ×10; scale bars, 100 μm; bone nodules appear as brownish black deposits on cell monolayer). (**H**) ALP expression was maintained in all groups of osteogenic GMSCs. (**I** to **K**) ARS was used to stain the mineralization of matrix in terms of calcium phosphate synthesis (ARS, red; magnification, ×10; scale bars, 100 μm), (**L**) which showed a significant decline in groups B and C as compared to group A (*$P < 0.05$, group A versus group B and group A versus group C). (**M** to **O**) GMSCs differentiated into neurons after induction for 21 days. Upon neurogenic induction, GMSCs from all the groups displayed similar expression of β-III tubulin (green, phalloidin; red, DAPI; blue, nuclei) and (**P** to **R**) nestin (red, phalloidin; green, DAPI; blue, nuclei), indicating that GMSCs have a skewed potential toward neuroectodermal differentiation (magnification, ×63; scale bars, 50 μm). (**S**) The graph displays average intensities of β-III tubulin and nestin. The average intensity was calculated after analyzing four different locations in a given sample (at ×40 magnification; fig. S1).

significant decrease in osteogenic cultures of groups B and C (Fig. 4L). As ALP is an early osteogenic marker, these observations imply that GMSCs from young and aging donors responded similarly to initial osteogenic stimulus (as depicted by similar ALP levels), but this tendency did not reach statistical significance, possibly due to high interindividual variations that are generally observed in differentiation assays (*23*, *39*). ALP is responsible for releasing phosphate and making it available for incorporation by the functional groups of bone matrix proteins. Therefore, the above observations advocate that GMSCs from all the age groups have similar potential for in vitro osteogenesis, but their ability to synthesize matrix proteins and to incorporate phosphate within the matrix at later stages of differentiation declines with age.

Unexpectedly, we did not observe any decline in neurogenic differentiation ability of GMSCs with donor age that was confirmed by the expression of β-III tubulin and nestin (Fig. 4, M to R). Immunostaining images at ×40 magnification were used to determine the MFI of both the neuronal markers, which did not display any significant difference (Fig. 4S and fig. S1). This unexpected aptitude toward neuronal lineage could be attributed to the fact that gingival tissues originate from the neural crest through the process of ectomesenchymal differentiation. Furthermore, gingiva has been detected to contain two subpopulations of MSCs including 90% neural crest–derived GMSCs and 10% mesoderm-derived GMSCs, out of which the neural crest–derived GMSCs showed an elevated potential for neuronal differentiation (*40*, *41*). On the basis of our findings and the previous reports, we suggest a skewed maturation of GMSCs toward neuronal lineage that is retained even with increasing age, whereas the tendency toward differentiation into mesodermal lineage and maturation declines with age.

To extrapolate our findings regarding the in vitro differentiation of GMSCs and to determine the applicability of GMSCs for bone tissue regeneration, we performed ectopic bone formation. Implantation of GMSC seeded hydroxyapatite collagen scaffolds in SCID (severe combined immunodeficient) mice revealed the presence of matrix proteins osteocalcin (Fig. 5, A to D) and collagen type I (Fig. 5, F to I), along with assimilation of calcium phosphate mineralization (Fig. 5, K to N). Scaffolds seeded with group B GMSCs showed significantly higher accumulation of osteocalcin than acellular scaffold (only scaffold) or scaffolds seeded with group A and C GMSCs (Fig. 5E). However, the levels of another matrix protein collagen type I decreased up to 30 to 40% in group B and C GMSCs as compared to group A (Fig. 5J), suggesting that although aging GMSCs responded to the osteogenic stimulus and differentiated into osteoblast, their capability to assimilate mineralized matrix declined with age. These findings were supported by the energy-dispersive spectroscopy (EDS) analysis of the recovered implants for calcium and phosphorus. As the assimilation of matrix proteins declined with the age of GMSCs undergoing in vivo osteogenesis, their potential to incorporate calcium phosphate for mineralization was also reduced significantly (Fig. 5O).

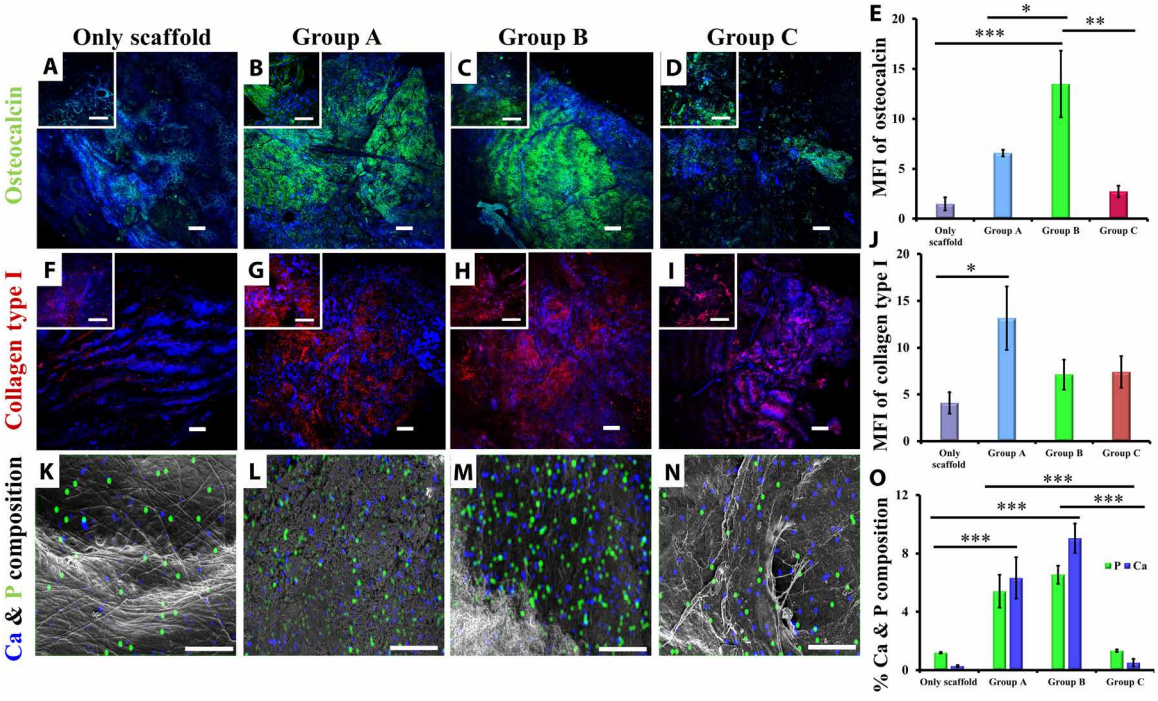

Fig. 5. Ectopic bone formation. Subcutaneous implantation of GMSC-seeded scaffold in SCID mice for 12 weeks resulted in osteogenic differentiation of GMSCs, as indicated by immunostaining for matrix proteins, (**A** to **D**) osteocalcin (green), and (**F** to **I**) collagen type I (red, pseudo-color) [magnification, ×60 (inset); scale bars, 100 μm; magnification, ×10; scale bars, 50 μm; nuclei, DAPI (blue)]. (**E**) Intensities of osteocalcin (***$P < 0.001$, only scaffold versus group B; **$P < 0.01$, group B versus group C; *$P < 0.05$, group A versus group B) and (**J**) collagen type I (*$P < 0.05$, only scaffold versus group A) were calculated from average intensities of ten random locations on retrieved implants, which indicated a decline in contribution of aging osteogenic GMSCs toward matrix mineralization. (**K** to **N**) Group C GMSCs displayed lower accumulation of calcium (blue) and phosphate (green) in implants as compared to implants seeded with group A and B GMSCs (magnification, ×1000; scale bars, 60 μm). (**O**) Quantitative analysis of Ca and P indicates significantly lower levels in scaffolds seeded with group C GMSCs (***$P < 0.001$; only scaffold versus group A; only scaffold versus group B; group A versus group C and group B versus group C). (A, F, and K) Acellular scaffolds (only scaffold) showed negligible levels of matrix proteins and mineralization.

Immunoregulatory behavior—Application for ALI

GMSCs suppress in vitro proliferation of PBMNCs, irrespective of donor age

To determine the immunomodulatory potential of GMSCs, a co-culture experiment of GMSCs with phytohemagglutinin (PHA)–stimulated peripheral blood mononuclear cells (PBMNCs) was carried out and the proliferation or survival of PBMNCs was determined. GMSCs from groups A, B, and C showed significant reduction in the in vitro proliferation of stimulated PBMNCs in a ratio of 1:7.5. GMSCs from group A displayed higher immunosuppressive potential, indicated by 75.86% reduction in PBMNC proliferation compared to stimulated PBMNCs, at 96 hours, whereas groups B and C displayed 60.74 and 64.45% reduction, respectively, at 96 hours (Fig. 6A). These findings suggest that although there is a slight decline in the immunosuppressive potential of aging GMSCs, it is not significant enough to reject their immunoregulatory behavior.

GMSCs reduce the inflammatory conditions and contribute toward regeneration of damaged lung tissue

The onset of an inflammatory lung condition is primarily investigated in relation to infiltration of neutrophils, up-regulation of pro-inflammatory cytokines, and several other degenerative changes. Intravenous administration of MSCs followed by their migration to

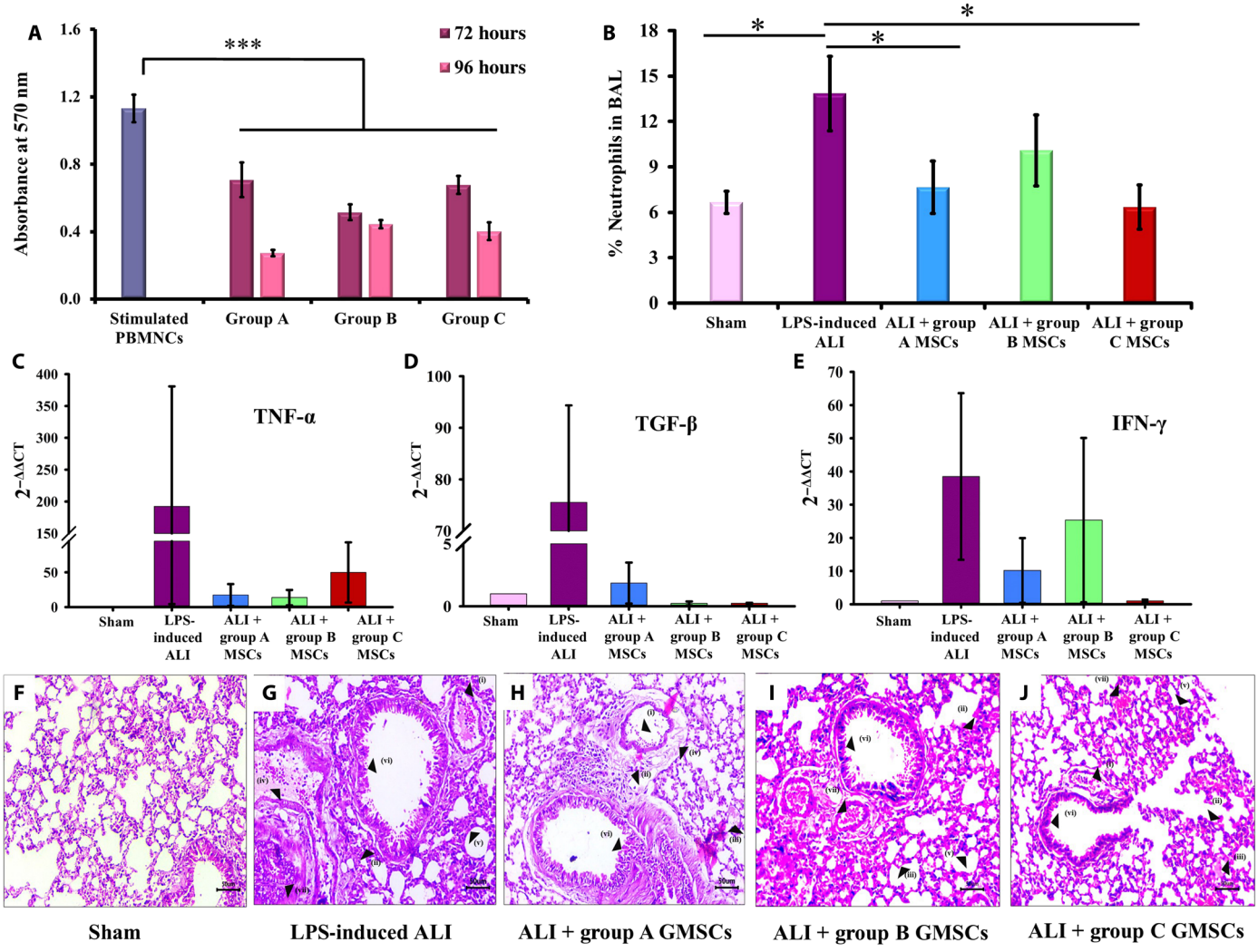

Fig. 6. In vitro and in vivo immunoregulation by GMSCs. (**A**) In vitro coculture of GMSCs with PHA-activated PBMNCs in a ratio of 1:7.5 demonstrated a significant suppression of PBMNC proliferation by all groups of GMSCs. Group A displayed maximum reduction at 96 hours (***$P < 0.001$, stimulated PBMNCs versus groups A, B, and C). (**B**) Mice with LPS administration displayed significantly high infiltration of neutrophils in BAL and lung tissue as compared to sham control. Intravenous administration of group A, B, and C GMSCs displayed reduction in the number of infiltrated neutrophils (*$P < 0.05$, sham versus LPS-induced ALI; LPS-induced ALI versus group A MSCs and LPS-induced ALI versus group C MSCs). (**C** to **E**) Induction of ALI by intranasal administration of LPS showed elevated gene levels of pro-inflammatory cytokines, TNF-α, TGF-β, and IFN-γ, in the cellular components of BAL as compared to sham control. Administration of group A, B, and C GMSCs has been found to reduce the expression levels of these pro-inflammatory cytokines. (**F** and **G**) Histological analysis of lung sections displayed indications of ALI in mice administered with LPS as compared to sham control. (**H** to **J**) A significant reduction in all the damage parameters was observed in mice administered with GMSCs from groups A, B, and C, resulting in improvement of overall lung health (magnification, ×20; scale bars, 50 μm; hematoxylin and eosin staining). Histological parameters studied (i) infiltration of neutrophils in alveoli and (ii) interstitial spaces; (iii) hyaline membrane formed due to fibrin polymerization that leaks into the interstitial/alveolar space; (iv) presence of proteinaceous debris in the alveolar space (such as fibrin strands); (v) thickening of alveolar septa; (vi) desquamation of alveolar epithelium; and (vii) thrombosis.

lung capillaries eventually leads to their entrapment in the lung spaces, where MSCs have been reported to immunoregulate the inflammatory environmental condition (*42*). In our experiments, we used LPS to generate lung inflammation and administered GMSCs from groups A, B, and C to investigate their in vivo immunosuppressive behavior. Flow cytometry analysis revealed a significantly high infiltration of granulocytes (neutrophils) in the animal group of LPS-induced ALI as compared to sham controls. Administration of group A and C GMSCs was observed to significantly reduce the neutrophil counts in LPS-induced ALI, thus exhibiting their high immunosuppressive potential (Fig. 6B).

In addition, GMSCs from groups A, B, and C also displayed down-regulation in gene expression of pro-inflammatory cytokines including tumor necrosis factor–α (TNF-α), transforming growth factor–β (TGF-β), and interferon-γ (IFN-γ; Fig. 6, C to E). As the decline in the levels of these cytokines was not significant, we suggest that mechanistic analysis at the level of signaling pathways could provide a better insight into the variation in behavior of GMSCs from different age groups. However, these variations in cell behavior can also be attributed to the employment of Swiss albino mice in our experiments, which provided a human relevant animal model in terms of genetic variability. Also, inclusion of cytokine profile would provide a better insight into the mechanisms involved in the regulation of pro-inflammatory cytokines.

Histopathological analysis of lung sections demonstrated extensive damage (in terms of infiltration of neutrophils in alveolar and interstitial spaces, thrombosis, presence of hyaline membrane, proteinaceous debris, and distorted alveolar septa) in mice induced with LPS resulting in ALI, as compared to sham control (Fig. 6, F and G). Administration of GMSCs in LPS-treated mice resulted in the reduction of infiltrated neutrophils in both alveolar and interstitial spaces; reduced the occurrence of hyaline membrane, proteinaceous debris, and thrombosis; and also promoted structural improvements in alveolar septa (Fig. 6, H to J). A detailed analysis of the histopathological sections is provided in Table 1. The above findings suggested that GMSCs from all the age group of donors ameliorated different (distinct) parameters of lung injury, indicating that if these GMSCs are implemented for stem cell therapy in human patients, they would be able to bring about improvement in overall lung health. While our experiments involved administration of single dose of GMSCs with a follow-up period of 4 days, we speculate that multiple rounds of administration followed by observations for longer duration would provide better insights into age-related immunoregulatory and regenerative behavior of GMSCs.

In addition to the above experiments, we also carried out similar study in adult age groups of mice (15 to 18 weeks and 27 to 30 weeks) and concluded that cellular behavior was largely dependent on the niche conditions of the recipient. In young mice, GMSCs from groups A, B, and C were found to bring about improvements in the overall health of damaged lung tissue. Whereas in adult and elderly age groups of mice we noticed that although GMSCs from groups B and C contributed in regenerating the damage caused by ALI, they did not exhibit in vivo immunosuppressive behavior. Both adult and elderly mice displayed varying parameters that represented severity of lung damage, but GMSCs from groups B and C were observed to alleviate all the concerned parameters to a certain extent (fig. S2 and table S1).

DISCUSSION

The coronavirus disease 2019 (COVID-19) pandemic has awakened the world to great consequences of biological risk and has reinstated the focus on health care research and safety management. Moreover, it also reiterated our attention toward the most vulnerable population of elderly individuals, as most of the economy of any country is devoted toward health care industry and elder care. This is because the comorbidities associated with age poses several hurdles to any treatment strategy designed for the old age individuals. Besides, immune senescence associated with aging increases the susceptibly of elderly people to various infections. Therefore, tailoring of cell-based therapies for older individuals has become inevitable for evolving personalized medicine and regenerative therapies (*42*).

Table 1. GMSC administration alleviates the severity of lung damage. Histological analysis of LPS-induced ALI in mice displayed different parameters of lung injury after LPS administration, followed by administration of GMSCs. Administration of GMSCs from groups A, B, and C was observed to alleviate all the parameters of ALI. "+" represents the presence of a given parameter in at least 10 random locations of a histological section. Eight such sections from different experimental animals of each group were analyzed to score the severity of lung damage. All the histological parameters were compared with sham control.

	Parameters of ALI	Sham control	LPS-induced ALI	LPS-induced ALI + group A GMSCs	LPS-induced ALI + group B GMSCs	LPS-induced ALI + group C GMSCs
(i)	Neutrophils in alveolar space	–	+++++	+++	+++	+++
(ii)	Neutrophils on interstitial space	–	+++++	+++	++	++
(iii)	Hyaline membrane	–	+++	+	+	+
(iv)	Proteinaceous debris	–	++	+	+	+
(v)	Thickening of alveolar septa	–	3×	2×	2.5×	2×
(vi)	Desquamation of alveolar epithelial cells	–	++	+	++	++
(vii)	Thrombosis	–	+++	+	++	+

The age-associated degenerative diseases demand regenerative therapeutic approaches to improve and comfort the lifestyle of elderly people. The main role of regenerative medicine is to replace and restore the normal function of cells, tissues, and organs that get damaged because of injury, trauma, or aging. In the past two decades, significant advancement in the field of stem cell research has revolutionized our approach toward regenerative medicine. In comparison to other candidates, MSCs have superior genetic stability and low risk of oncologic issues (due to spontaneous transformation) following transplantation (*1*, *11*, *22*). Extensive research on stem cell sources including BM, AT, DP, muscles, umbilical cord blood, and endometrium has established cell-based tissue engineering approaches as the most promising course of action for degenerative diseases. However, a decline in stem cell yield and function with age hampers their suitability for autologous cell therapy. Although dental tissues present themselves as an accessible option, the lack of substantial age-related research on dental stem cells restricts their clinical appreciation.

Our study emphasizes on studying the biological properties of one such dental tissue—gingiva—and highlights its stem cell properties in relation to donor age. In addition to its ecto-mesenchymal origin, the gingival connective tissue shows a unique developmental pattern in terms of its genesis partly from the perifollicular mesenchyme (the outer layer of dental follicle) and partly from the dental follicle proper (the inner layer of dental follicle) (*23*, *40*, *41*). This phenomenon imparts uniqueness to gingival tissue in terms of embodying heterogeneous cell population (two subpopulations: neural crest–derived GMSCs and mesoderm-derived GMSCs) that exhibit distinctive stem cell properties and variable responses to growth factors and stress conditions *(23*, *40*, *41*, *43*). Some of the previous reports demonstrating deleterious effects of aging on GMSC proliferation and migration do not consider this diversity in population (*44*, *45*). Besides, there are no reports related to the effect of age on the phenotypic, growth, functional, and immunoregulatory behaviors of GMSCs. Ours is the first report to investigate the donor age–related evaluation of GMSCs for their utility in regenerative medicine.

Our findings provide three important insights. The first is related to the possibility of isolating large quantities of GMSCs from donors of all ages, including adults up to 80 years of age. In contrast to fetal development, which witnesses rapid stem cell division, adulthood is associated with slowing down or quiescence of cell division, merely for the purpose of maintaining tissue homeostasis (*30*, *46*). In case of dental tissues, DP seems to have the highest turnover rate, as illustrated by eruption and re-eruption of tooth until 14 to 15 years of age. In comparison to DP, periodontal tissues such as PDL and gingiva remain quiescent and maintain an undifferentiated yet committed state similar to skeletal stem cells (*47*, *48*), suggesting conservation of stem cell pool in terms of quantity and/or quality. In relation to this, we observed that the cellular morphology, colony formation efficiency, rate of proliferation, number of in vitro doublings, and the expression of MSC surface markers are maintained independent of donor age (primarily during early passages, as late passages involve in vitro replicative senescence). A similar report related to DP demonstrated that MSCs display an optimum growth and phenotypic characteristics irrespective of the age of donor. However, the performance of these cells is contradictory under in vitro and in vivo microenvironments (*16*).

Many previous studies have highlighted that gingival tissues are constantly under stress due to frequent exposure to bacterial insults resulting in gingival inflammation (*26*, *27*). Consequently, GMSCs exhibit higher levels of growth factor receptors that assist in enhanced cellular proliferation and maintenance of tissue homeostasis (*46*, *49*). An associated enhancement in the expression of PDGFR, FGFR, and EGFR in our experiments supported the above reports about sustenance of gingival health under the conditions of frequent microbial insults and increasing inflammatory environment with age (*49*–*52*). Nevertheless, we observed higher senescent population and increase in PDT of GMSCs derived from elderly donors, which signify impairment in stemness due to extensive in vitro passaging, although the rate of in vitro senescence in old GMSCs is slower as compared to their young counterparts. The above findings resonate with the previous report suggesting existence of several subpopulations in a given culture (*9*). The in vitro population of GMSCs is composed of subsets of young and senescing population that is visible by the variable numbers of SA-β-gal^{+ve} cells in group C. The senescing cell fate might guide GMSCs to either apoptosis or autophagy. Activation of both these mechanisms supports maintenance of healthy stem cell pool. Consequently, in our experiments, a higher expression of p53, SIRT1, and CDKN2A suggested an efficient DNA damage response and lower possibilities of senescence-associated tumorigenicity (*14*, *30*, *53*–*55*). Besides, elevated p53 and SIRT1 contribute toward maintenance of gingival tissue homeostasis by averting tumorigenic events through apoptosis or autophagy, respectively, and the resulting decline in cell numbers is compensated by enhancement in the expression of growth factor receptors.

The second insight relates to a skewed differentiation of GMSCs toward neuronal lineage, irrespective of age, suggesting that a stem cell therapy using GMSCs would perform better in treatment strategies that require neuronal regeneration. Furthermore, even undifferentiated GMSCs expressed neural stem cell markers. This inclination toward ectodermal lineage can be correlated to the evolutionary history and physiology of gingiva (*56*), which highlights that gingiva serves as an important reservoir of neural crest–derived stem cells that exhibit aptitude toward both mesodermal and ectodermal differentiation (*23*). However, in vitro commitment toward mesenchymal lineage (osteogenic and adipogenic) was observed to decline with age. This variance in responsiveness to differentiation factors validates earlier claim that gingival tissue embodies a heterogeneous cell population (*40*) and the fact that microenvironmental conditions play an important role in governing cellular behavior (*49*). In relation to this, some of the earlier reports state that the function of hematopoietic stem cells (HSCs) deteriorates with age, without any decline in HSC numbers (*2*), whereas some cells with very high metabolic activity (such as cortical neurons and cardiomyocytes) never get replaced during lifetime (*2*). Evidently, our findings also indicate that the microenvironmental cues for stem cell proliferation and differentiation are entirely different and act independent of each other.

The above statements are supported by our ectopic bone formation experiment, which validates variation in cellular behavior under in vitro and in vivo conditions, and also support the role of microenvironmental cues (*16*). Although subcutaneous implantation of GMSC-seeded implants at an ectopic site ensures no interference due to indigenous cells of bone and also ascertains osteogenesis purely due to differentiation of GMSCs into mature osteoblasts, it does not accurately replicate the microenvironment of bone. In addition, because of the absence of conditions similar to the original niche, some

of the matrix proteins behave abnormally and do not contribute to conclusive data, but this does not warrant a decline in regenerative potential of GMSCs with donor age.

Studies related to regenerative potential of MSCs reveal that MSCs suppress the overactivated immune system and promote endogenous repair by improving the microenvironment. MSCs have also been found to be nonpermissive to SARS-CoV-2 (severe acute respiratory syndrome coronavirus 2) infection, which support their growing demand as a potential therapeutic option for COVID-19 (*57*, *58*). Our third insight intends to propose GMSCs as a potential treatment option for such inflammatory conditions, for which we examined how age governs the immunoregulatory behavior of GMSCs in the LPS-induced ALI model. We observed that parameters such as increased infiltration of neutrophils in alveolar and interstitial space, accompanied by thickening of alveolar septa, thrombosis, accumulation of proteinaceous debris, and desquamation of alveolar epithelium, attribute to the severity of lung infection (*59*, *60*). Intravenous administration of group A, B, and C GMSCs demonstrated alleviation in most of the parameters mentioned above, indicating an efficient anti-inflammatory and regenerative response. Our supplementary data that involve administration of group B and C GMSCs in adult (age, 15 to 18 weeks) and elderly (age, 27 to 30 weeks) mice depicted that aging GMSCs generate regenerative changes in the recipient mice but fall short in achieving suppression of the inflammatory lung environment. These findings encourage us to postulate that complete recovery might require administration of multiple doses of GMSCs, followed by long-term follow-ups. Thus, we conclude that both the age-related changes in cellular behavior and local microenvironmental conditions should be taken into consideration while studying the effect of age on cell-based regenerative therapeutic approaches.

Aged GMSCs function in a cell-autonomous manner under in vitro culture conditions, but their interactions with the niche and the microenvironment that they encounter after transplantation are bidirectional. Therefore, alterations in the niche as a consequence of natural aging affect the survival and integration of transplanted cells. Most of our present understanding and elucidation models originate from in vitro cell culture systems and in vivo animal models, which do not translate into human clinical situations entirely. Therefore, designing a stem cell therapy requires a more comprehensive approach to investigate and analyze the variability in the host microenvironment, as favorable cues from the niche govern the success of any therapy. Our data highlight one such detailed investigation about a less studied source of MSCs—gingiva—and explore their utility as a treatment option for acute inflammatory lung conditions such as COVID-19.

MATERIALS AND METHODS

Harvesting of gingival tissues

Gingival tissues were harvested from healthy individuals during gingivectomy or tooth extraction procedures without prognosis. The samples were harvested after receiving written informed consent from healthy donors and were categorized into three age groups: group A (13 to 31 years; mean age ± SD, 23.29 ± 6.26 years; $n = 14$), group B (37 to 55 years; mean age ± SD, 45.69 ± 6.49 years; $n = 13$), and group C (59 to 80 years; mean age ± SD, 65.36 ± 6.57 years; $n = 14$) (Fig. 1A). The gingival samples were harvested under aseptic conditions, transported to the laboratory on ice, in maintenance medium, and processed within 2 hours.

Ethics statement

The protocol for this study was approved by the Institutional Ethics Committees of Deenanath Mangeshkar Hospital and Research Centre, Pune, India and Savitribai Phule Pune University, Pune, India. Written informed consent was received from all the participants.

Isolation and expansion of GMSCs

The gingival tissues were de-epithelialized and treated enzymatically to obtain single-cell suspension, as described previously (*22*). The cells were maintained in α modification of minimum essential medium (Sigma-Aldrich, UK) supplemented with 10% fetal bovine serum (FBS) (Gibco, USA) and incubated at 37°C in 5% CO_2. The confluent cultures were subcultured using trypsin phosphate versene glucose [TPVG; 0.1% trypsin, 0.02% EDTA, 0.05% glucose in Dulbecco's phosphate-buffered saline (PBS); HiMedia, India], and the experiments were performed using cells between passages 3 and 7 (unless specified). Cell viability was estimated after each passage by trypan blue exclusion method.

Colony formation and growth kinetics

The colony formation assay was performed by seeding the limiting dilution of GMSCs at a density of 10 cells/cm^2. The cultures were then incubated at 37°C in 5% CO_2 for 7 days. The nutrient medium was changed every second day. After 7 days, the cultures were fixed using 3.7% paraformaldehyde (PFA) for 15 min at 4°C and then stained with 1% eosin (HiMedia, India) for 20 min. The cell clusters with aggregates of 50 or more cells were scored as a colony and counted as a colony-forming unit–fibroblast (CFU-f).

MTT assay was performed to compare the proliferation rates of GMSCs. Briefly, 10^4 cells per well were seeded in a 96-well plate, and MTT assay was performed after 24 and 48 hours of incubation. Absorbance at 570 nm was determined, which represented the amount of conversion of MTT to formazan by mitochondrial dehydrogenase, suggesting cell viability/proliferation.

To assess the PDT of GMSCs, cells between passages 9 and 13 were seeded in a T-25 flask at a seeding density of 2×10^5 cells and incubated at 37°C in 5% CO_2 for 96 hours. After 96 hours, the cells were harvested using TPVG and counted by trypan blue exclusion method. PDT was calculated as follows

$$\text{PDT (hours)} = \text{duration of experiment} \times \frac{\log 2}{\log\left(\frac{\text{no. of cells harvested}}{\text{no. of cells seeded}}\right)}$$

The number of cell doublings was determined by using the following formula

$$\text{Population doublings (PD)} = \frac{\log\left(\frac{\text{no. of cells harvested}}{\text{no. of cells seeded}}\right)}{\log 2}$$

Surface marker analysis by flow cytometry

The phenotypic characterization of GMSCs for MSC surface marker expression was carried out using flow cytometry. Briefly, cells of passages 2 to 10 were trypsinized, fixed with 3.7% PFA for 15 min at 4°C, and blocked with 10% FBS for 45 min at 4°C. Cell aliquots were then incubated with fluorochrome-labeled MSC CD markers including anti-human CD44, CD90 (BD Biosciences, USA), CD73, CD105 (eBioscience, USA), CD34, and CD45 (HSC markers; BD

Biosciences, USA) antibodies and their respective isotype controls (all at a dilution of 1:100) for 45 min at 4°C. Labeled cells were acquired using BD FACSVerse and analyzed using FACSuite Software (BD Biosciences, USA). The percentage of cells expressing the MSC surface markers and the MFI of each marker were calculated and considered for analysis (MFI of the surface antigen was normalized with its respective isotype control).

SA-β-gal assay

β-Gal present in the senescent cells cleaves X-galactosidase (X-Gal) into 5,5′-dibromo-4,4′-dichloro-indigo, which produces a distinct green-blue color. In brief, GMSCs between passages 4 to 6 (early passages) and 9 to 12 (late passages) were seeded into a six-well plate at a density of 10^4 cells per well and incubated at 37°C in 5% CO_2. After 4 days, they were fixed using 3.7% PFA for 15 min at 4°C. The staining was performed with 0.1% X-Gal and staining solution (pH 6) at 37°C for 24 hours (*61*). The reaction was stopped by giving washes of distilled water, and the number of SA-β-gal^{+ve} cells was counted under a phase contrast microscope (Magnus, Olympus, India).

Real-time PCR

For real-time polymerase chain reaction (PCR), a 10-μl reaction was set up with GoTaq qPCR Master Mix (Promega, USA), along with complementary DNA (cDNA) and 10 pmol of gene-specific primers. The primer sequences used are shown in table S2. Real-time PCR was set using StepOnePlus System (Applied Biosystems, USA). The amplification was performed using 1 cycle of 95°C for 2 min and 40 cycles of 95°C for 15 s and 60°C for 60 s, followed by melt curve analysis. The relative gene expression was calculated by using the $2^{-\Delta\Delta CT}$ method.

Cell migration assay

To determine the migration ability of GMSCs for in vitro wound healing, scratch assay was performed. GMSCs were seeded at a density of 2×10^4 cells per well in a six-well plate, and the cells were allowed to grow until confluency. A wound was created in the monolayer culture using a micropipette tip, and migration of cells was recorded until 48 hours. The images at each time point were captured using a phase contrast microscope and analyzed with Fiji ImageJ software (*62*). The percent wound healing was calculated as follows

$$\%\text{Wound closure} = \frac{\text{Initial area of wound} - \text{Area of wound after "X" hour}}{\text{Initial area of wound}} \times 100$$

In vitro differentiation of GMSCs

GMSCs have been demonstrated to undergo osteogenic, chondrogenic, adipogenic, and neurogenic differentiation by previous researchers (*22*–*24*). In our experiments, we aimed at studying the effect of age on the multidifferentiation potential of GMSCs. We stimulated GMSCs from each group with adipogenic, neurogenic, and osteogenic inductions. For each of these experiments, 2×10^4 cells per well were seeded in a 24-well plate.

Adipogenesis

The confluent monolayer cultures of GMSCs were induced with adipogenic induction medium for 3 days, followed by incubation in maintenance medium for 1 day (Adipogenic Differentiation Kit, Lonza, Switzerland). After seven cycles of induction and maintenance, the cells were washed with PBS and fixed with 10% formalin for 1 hour at room temperature. The oil globules accumulated by cells were stained using Oil Red O (3 mg/ml; Sigma-Aldrich, UK) for 1 hour at 37°C, after which they appeared red. The stained cells were observed under a phase contrast microscope, and the number of cells that had accumulated the oil globules was microscopically quantitated.

Osteogenesis

GMSCs were subjected to osteogenic stimuli in the presence of StemPro Osteogenic induction medium (Gibco, USA). After 21 days, the cultures were fixed with 3.7% PFA at 4°C for 15 min and stained with 40 mM ARS (Sigma-Aldrich, UK) to detect the synthesis of mineralized matrix. The bone nodules and the ARS-stained cultures were observed under a phase contrast microscope, and images were captured. The ARS stain was extracted using 10% acetic acid, and the extracts were heated at 85°C for 10 min. It was then centrifuged, and the supernatant was neutralized with 10% ammonium hydroxide. The absorbance was measured at 405 nm to quantitate ARS from the osteogenic cultures. The standard graph was plotted using serial dilutions of ARS in acetic acid.

ALP is an early marker for osteogenic differentiation, and therefore, quantification of ALP was carried out at day 5 of osteogenic induction to determine the effect of aging on the osteogenic potential of GMSCs. For determining ALP concentration, osteogenically stimulated GMSCs were harvested and cell lysates were prepared in 0.1% Triton X-100. These were incubated with para-nitro phenol phosphate (3.75 μg/μl; SRL, India) containing 1.5 mM $MgCl_2$ and AMP (2-amino 2-methyl 1-propanol, pH 10.5; Sigma-Aldrich, UK) for 30 min at 37°C. The reaction was stopped by addition of 1 N NaOH, and the absorbance was measured at 405 nm. The standard graph was prepared using serial dilutions of para-nitro phenol (Sigma-Aldrich, UK) in NaOH.

Neurogenesis

The tissue culture vessel used for neurogenic induction was precoated with 5 μg of laminin (Invitrogen, USA) and 5 μg of poly-D-lysine (MP Biomedicals, India). The confluent monolayer cultures of GMSCs were incubated with DMEM-F12 (Gibco, USA) supplemented with FGF-2 (10 ng/ml; Gibco, USA), EGF (Gibco, USA), and 1× N2 supplement (Gibco, USA) for 25 days. The neuronal differentiation was found to be associated with rosette formation at 10 to 14 days of differentiation cycle. After 25 days, the cells were fixed with 3.7% PFA at 4°C for 15 min, permeabilized with 0.1% Triton X-100, and blocked with 10% FBS for 1 hour. This was followed by incubation with anti-human nestin conjugated with Alexa Fluor 555 (dilution 1:200) or anti-human β-III tubulin antibodies (dilution 1:300) (Invitrogen, USA) for 2 hours. Goat anti-mouse fluorescein isothiocyanate (FITC) antibody (Invitrogen, USA; dilution 1:100) was used as the secondary antibody for β-III tubulin. Phalloidin FITC (Sigma-Aldrich, UK) and rhodamine phalloidin (Invitrogen, USA) were used to stain the cytoskeleton. After staining, the cells were mounted in Ultra Cruz mounting medium containing 4′,6-diamidino-2-phenylindole (DAPI; Santa Cruz Biotechnology, USA) and observed under 40× and 63× oil immersion objectives (Leica SP5 II, Germany). Images were analyzed using Fiji ImageJ software. The average intensities of β-III tubulin and nestin were determined by using four different locations in a given sample at ×40 magnification.

Ectopic bone formation

Cells (10^6) from group A, B, and C GMSCs were seeded on hydroxyapatite collagen scaffolds and induced with osteogenic induction medium. After 10 days of osteogenic stimulus, the scaffolds with or without cells were implanted ectopically in the subcutaneous pockets of BALB/c SCID mice (6 to 8 weeks, male). Scaffolds without cells were used as negative controls. Implants were recovered from the mice after 12 weeks and analyzed for the presence of bone matrix proteins.

The recovered implants were stained with anti-human osteocalcin and collagen type I antibodies (Abcam, UK) at a dilution of 1:200. Donkey anti-rabbit FITC (Santa Cruz Biotechnology, USA) was used as the secondary antibody at a dilution of 1:100, and the implants were mounted in Ultra Cruz mounting medium containing DAPI (Santa Cruz Biotechnology, USA). Ten different regions of the samples were observed under 10× and 60× (oil) objectives (Nikon A1 R, Japan), and MFIs were calculated using Fiji ImageJ software.

The recovered implants were also processed for scanning electron microscopy (FEI Nova NanoSEM 450) to determine the percent elemental composition by EDS (Bruker XFlash 6I30). The implants were fixed in 3.7% PFA at 4°C for 15 min and dehydrated using serial dilutions of ethanol. These were sputter-coated with Au, and the elemental composition of calcium and phosphorus was recorded using EDS at 10 different locations on the scaffold.

Coculture of GMSCs with PBMNCs

GMSCs have been known to exhibit immunomodulatory properties under a variety of chronic and acute inflammatory conditions (*23*, *25*, *27*, *63*). To determine the effect of age on immunomodulatory behavior of GMSCs, we studied the interactions of GMSCs from groups A, B, and C with PHA (Sigma-Aldrich, UK)–stimulated PBMNCs, as per the standard protocol (*64*, *65*). PBMNCs were isolated from human blood by Ficoll (Histopaque; Sigma-Aldrich, UK) density gradient centrifugation. The blood collection and processing protocol was approved by the Institutional Ethics Committee of the Savitribai Phule Pune University. Written informed consent was received from all the donors. GMSCs were seeded in a 96-well plate and allowed to adhere for 24 hours. PBMNCs were stimulated with PHA (5 μg/ml) and cocultured with γ-irradiated (30 Gy, 16.58 min; Gamma Chamber GC-5000) GMSCs. The gamma irradiation stagnated the proliferation of GMSCs but did not affect their function. The experiments were conducted with GMSC:PBMNC ratios of 1:7.5, 1:12.5, 1:15, 1:25, and 1:50. After 72 and 96 hours of coculture, the proliferation of stimulated PBMNCs was evaluated by MTT assay.

GMSC treatment in LPS-induced ALI model

In addition, we investigated the consequences of donor age on the immunomodulatory properties of GMSCs, using LPS-induced ALI in mouse model as described in earlier report (*42*). Many of the previous reports have studied the anti-inflammatory properties of human MSCs in a mouse model of inflammatory diseases including colitis, atherosclerosis, and acute respiratory distress syndrome (*25*–*27*, *42*). Our experimental model involved intranasal administration of LPS at a concentration of 5 μg/g body weight in Swiss albino mice (6 to 8 weeks, male). Sham control was intranasally administered with PBS. After 72 hours of LPS administration, GMSCs from groups A, B, and C (10^6 cells per mouse) were injected intravenously. Sham group was injected with PBS. The experiment was conducted in triplicate with three individual samples from each group of GMSCs (four animals per sample, a total of 12 animals for each age group of GMSCs). The experiment was terminated after 96 hours of GMSC administration, by sacrificing the experimental animals and analyzing their lung tissues. The protocol for the above experiment involved humane care and was approved by the Institutional Animal Ethics Committee of Preclinical Research and Development Organization (PRADO) Pvt. Ltd., Pune.

An increase in the numbers of infiltrated neutrophils and enhanced concentrations of pro-inflammatory cytokines in the lung tissues and bronchoalveolar lavage (BAL) gives a relevant measurement of the inflammatory response (*59*, *60*). Therefore, we collected BAL and harvested lungs for further analysis. BAL was centrifuged at 2000 rpm for 15 min to separate the cells and the pulmonary supernatant. The cellular component was analyzed using flow cytometry to determine the percentage of infiltrated neutrophils. In addition to BAL, single-cell suspension of whole lung was also studied by flow cytometry for the presence of neutrophils in the lung tissue. The neutrophil (granulocyte) population was gated on the basis of scatterplot analysis (*66*).

The cellular component of BAL was subjected to real-time PCR to determine the regulation of gene expression of pro-inflammatory cytokines. Ten-microliter reaction was set up with PowerUp SYBR Green Master Mix (Applied Biosystems, USA), along with cDNA and 10 pmol of gene-specific primers. The primer sequences used are shown in table S2. Real-time PCR was set up using StepOnePlus System (Applied Biosystems, USA). The amplification was performed using 1 cycle of 95°C for 10 min and 40 cycles of 95°C for 15 s and 60°C for 60 s, followed by melt curve analysis. The relative gene expression was calculated by using the $2^{-\Delta\Delta CT}$ method. The gene expression profiles of GMSC administered mice were normalized with the sham control.

For histopathological analysis, mouse lungs were fixed in 4% formalin and embedded in paraffin, sectioned, and stained with hematoxylin and eosin to score inflammation. The histological analysis was carried out by a double-blind method, and the sections were observed under a bright-field microscope (Magnus, Olympus, India) for scoring the following parameters: (i) infiltration of neutrophils in alveoli and (ii) interstitial spaces; (iii) hyaline membrane formed due to fibrin polymerization that leaks into the interstitial/alveolar space; (iv) presence of proteinaceous debris in the alveolar space (such as fibrin strands); (v) thickening of alveolar septa; (vi) desquamation of alveolar epithelium; and (vii) thrombosis (*59*, *60*).

Statistics

For each experiment, we used GMSCs from five random samples between passages 3 and 7 (unless specified) from each age group. Every experiment was conducted in triplicate, and the statistical analysis was carried out using SigmaPlot 13. One-way analysis of variance (ANOVA) was performed with all pairwise multiple comparison procedures or versus control (Holm-Sidak method) to evaluate statistical significance (*$P < 0.05$, **$P < 0.01$, and ***$P < 0.001$). Data are represented as means, with error bars indicating the SE/SD (as specified).

SUPPLEMENTARY MATERIALS

Supplementary material for this article is available at https://science.org/doi/10.1126/sciadv.abm6504

View/request a protocol for this paper from *Bio-protocol*.

REFERENCES AND NOTES

1. F. Z. Asumda, Age-associated changes in the ecological niche: Implications for mesenchymal stem cell aging. *Stem Cell Res. Ther.* **4**, 47 (2013).
2. J. F. De Mora, A. D. Juan, The decay of stem cell nourishment at the niche. *Rejuvenation Res.* **16**, 487–494 (2013).
3. D. Ma, Z. Ma, X. Zhang, W. Wang, Z. Yang, M. Zhang, G. Wu, W. Lu, Z. Deng, Y. Jin, Effect of age and extrinsic microenvironment on the proliferation and osteogenic differentiation of rat dental pulp stem cells in vitro. *J. Endod.* **35**, 1546–1553 (2009).
4. K. Iohara, M. Murakami, K. Nakata, M. Nakashima, Age-dependent decline in dental pulp regeneration after pulpectomy in dogs. *Exp. Gerontol.* **52**, 39–45 (2014).
5. H. Alzer, H. Kalbouneh, F. Alsoleihat, N. Abu Shahin, S. Ryalat, M. Alsalem, H. Alahmad, L. Tahtamouni, Age of the donor affects the nature of in vitro cultured human dental pulp stem cells. *Saudi Dent. J.* **33**, 524–532 (2021).
6. R. X. Wu, C. S. Bi, Y. Yu, L. L. Zhang, F. M. Chen, Age-related decline in the matrix contents and functional properties of human periodontal ligament stem cell sheets. *Acta Biomater.* **22**, 70–82 (2015).
7. O. Katsara, L. G. Mahaira, E. G. Iliopoulou, A. Moustaki, A. Antsaklis, D. Loutradis, K. Stefanidis, C. N. Baxevanis, M. Papamichail, S. A. Perez, Effects of donor age, gender, and in vitro cellular aging on the phenotypic, functional, and molecular characteristics of mouse bone marrow-derived mesenchymal stem cells. *Stem Cells Dev.* **20**, 1549–1561 (2011).
8. M. Zaim, S. Karaman, G. Cetin, S. Isik, Donor age and long-term culture affect differentiation and proliferation of human bone marrow mesenchymal stem cells. *Ann. Hematol.* **91**, 1175–1186 (2012).
9. T. J. Block, M. Marinkovic, O. N. Tran, A. O. Gonzalez, A. Marshall, D. D. Dean, X. D. Chen, Restoring the quantity and quality of elderly human mesenchymal stem cells for autologous cell-based therapies. *Stem Cell Res. Ther.* **8**, 239 (2017).
10. X. Ye, C. Liao, G. Liu, Y. Xu, J. Tan, Z. Song, Age-related changes in the regenerative potential of adipose-derived stem cells isolated from the prominent fat pads in human lower eyelids. *PLOS ONE* **11**, e0166590 (2016).
11. M. S. Choudhery, M. Badowski, A. Muise, J. Pierce, D. T. Harris, Donor age negatively impacts adipose tissue-derived mesenchymal stem cell expansion and differentiation. *J. Transl. Med.* **12**, 8 (2014).
12. E. U. Alt, C. Senst, S. N. Murthy, D. P. Slakey, C. L. Dupin, A. E. Chaffin, P. J. Kadowitz, R. Izadpanah, Aging alters tissue resident mesenchymal stem cell properties. *Stem Cell Res.* **8**, 215–225 (2012).
13. J. S. Jung, C. Volk, C. Marga, A. Navarrete Santos, M. Jung, D. Rujescu, A. Navarrete Santos, Adipose-derived stem/stromal cells recapitulate aging biomarkers and show reduced stem cell plasticity affecting their adipogenic differentiation capacity. *Cell. Reprogram.* **21**, 187–199 (2019).
14. I. Iezzi, P. Pagella, M. Mattioli-Belmonte, T. A. Mitsiadis, The effects of ageing on dental pulp stem cells, the tooth longevity elixir. *Eur. Cells Mater.* **37**, 175–185 (2019).
15. B. M. Schipper, K. G. Marra, W. Zhang, A. D. Donnenberg, J. P. Rubin, Regional anatomic and age effects on cell function of human adipose-derived stem cells. *Ann. Plast. Surg.* **60**, 538–544 (2008).
16. E. Bressan, L. Ferroni, C. Gardin, P. Pinton, E. Stellini, D. Botticelli, S. Sivolella, B. Zavan, Donor age-related biological properties of human dental pulp stem cells change in nanostructured scaffolds. *PLOS ONE* **7**, e49146 (2012).
17. D. Zhang, S. He, Q. Wang, S. Pu, Z. Zhou, Q. Wu, Impact of aging on the characterization of brown and white adipose tissue-derived stem cells in mice. *Cells Tissues Organs* **209**, 26–36 (2020).
18. A. Wilson, L. A. Shehadeh, H. Yu, K. A. Webster, Age-related molecular genetic changes of murine bone marrow mesenchymal stem cells. *BMC Genomics* **11**, 229 (2010).
19. R. B. Özgül Özdemir, A. T. Özdemir, C. Kırmaz, A. Eker Sarıboyacı, E. Karaöz, G. Erman, H. S. Vatansever, N. Mete Gökmen, Age-related changes in the immunomodulatory effects of human dental pulp derived mesenchymal stem cells on the $CD4^+$ T cell subsets. *Cytokine* **138**, 155367 (2021).
20. C. Fan, Q. Ji, C. Zhang, S. Xu, H. Sun, Z. Li, TGF-β induces periodontal ligament stem cell senescence through increase of ROS production. *Mol. Med. Rep.* **20**, 3123–3130 (2019).
21. J. Zhang, Y. An, L.-N. Gao, Y.-J. Zhang, Y. Jin, F.-M. Chen, The effect of aging on the pluripotential capacity and regenerative potential of human periodontal ligament stem cells. *Biomaterials* **33**, 6974–6986 (2012).
22. G. B. Tomar, R. K. Srivastava, N. Gupta, A. P. Barhanpurkar, S. T. Pote, H. M. Jhaveri, G. C. Mishra, M. R. Wani, Human gingiva-derived mesenchymal stem cells are superior to bone marrow-derived mesenchymal stem cells for cell therapy in regenerative medicine. *Biochem. Biophys. Res. Commun.* **393**, 377–383 (2010).
23. D. Kim, A. E. Lee, Q. Xu, Q. Zhang, A. D. Le, Gingiva-derived mesenchymal stem cells: Potential application in tissue engineering and regenerative medicine—A comprehensive review. *Front. Immunol.* **12**, 667221 (2021).
24. X. L. Fan, Y. Zhang, X. Li, Q. L. Fu, Mechanisms underlying the protective effects of mesenchymal stem cell-based therapy. *Cell. Mol. Life Sci.* **77**, 2771–2794 (2020).
25. Q. Zhang, S. Shi, Y. Liu, J. Uyanne, Y. Shi, S. Shi, A. D. Le, Mesenchymal stem cells derived from human gingiva are capable of immunomodulatory functions and ameliorate inflammation-related tissue destruction in experimental colitis. *J. Immunol.* **184**, 1656 (2010).
26. P. Ahangar, S. J. Mills, L. E. Smith, S. Gronthos, A. J. Cowin, Human gingival fibroblast secretome accelerates wound healing through anti-inflammatory and pro-angiogenic mechanisms. *npj Regen. Med.* **5**, 24 (2020).
27. X. Zhang, F. Huang, W. Li, J. L. Dang, J. Yuan, J. Wang, D. L. Zeng, C. X. Sun, Y. Y. Liu, Q. Ao, H. Tan, W. Su, X. Qian, N. Olsen, S. G. Zheng, Human gingiva-derived mesenchymal stem cells modulate monocytes/macrophages and alleviate atherosclerosis. *Front. Immunol.* **9**, 878 (2018).
28. M. A. Baxter, R. F. Wynn, S. N. Jowitt, J. E. Wraith, L. J. Fairbairn, I. Bellantuono, Study of telomere length reveals rapid aging of human marrow stromal cells following in vitro expansion. *Stem Cells* **22**, 675–682 (2004).
29. L. García-Prat, P. Muñoz-Cánoves, Aging, metabolism and stem cells: Spotlight on muscle stem cells. *Mol. Cell. Endocrinol.* **445**, 109–117 (2017).
30. R. A. J. Signer, S. J. Morrison, Mechanisms that regulate stem cell aging and life span. *Cell Stem Cell* **12**, 152–165 (2013).
31. A. Krtolica, Stem cell: Balancing aging and cancer. *Int. J. Biochem. Cell Biol.* **37**, 935–941 (2005).
32. D. Dufrane, Impact of age on human adipose stem cells for bone tissue engineering. *Cell Transplant.* **26**, 1496–1504 (2017).
33. A. Sanghani-Kerai, L. Osagie-Clouard, G. Blunn, M. Coathup, The influence of age and osteoporosis on bone marrow stem cells from rats. *Bone Jt. Res.* **7**, 289–297 (2018).
34. M. Liu, H. Lei, P. Dong, X. Fu, Z. Yang, Y. Yang, J. Ma, X. Liu, Y. Cao, R. Xiao, Adipose-derived mesenchymal stem cells from the elderly exhibit decreased migration and differentiation abilities with senescent properties. *Cell Transplant.* **26**, 1505–1519 (2017).
35. Q. Li, Y. Ma, Y. Zhu, T. Zhang, Y. Zhou, Declined expression of histone deacetylase 6 contributes to periodontal ligament stem cell aging. *J. Periodontol.* **88**, e12–e23 (2017).
36. W. Zheng, S. Wang, D. Ma, L. Tang, Y. Duan, Y. Jin, Loss of proliferation and differentiation capacity of aged human periodontal ligament stem cells and rejuvenation by exposure to the young extrinsic environment. *Tissue Eng. Part A* **15**, 2363–2371 (2009).
37. J. Campisi, L. Robert, Cell senescence: Role in aging and age-related diseases. *Aging* **39**, 45–61 (2014).
38. M. Khorraminejad-Shirazi, M. Dorvash, A. Estedlal, A. H. Hoveidaei, M. Mazloomrezaei, P. Mosaddeghi, Aging: A cell source limiting factor in tissue engineering. *World J. Stem Cells* **11**, 787–802 (2019).
39. G. Kasper, L. Mao, S. Geissler, A. Draycheva, J. Trippens, J. Kühnisch, M. Tschirschmann, K. Kaspar, C. Perka, G. N. Duda, J. Klose, Insights into mesenchymal stem cell aging: Involvement of antioxidant defense and actin cytoskeleton. *Stem Cells* **27**, 1288–1297 (2009).
40. K. M. Fawzy El-Sayed, C. E. Dörfer, Gingival mesenchymal stem/progenitor cells: A unique tissue engineering gem. *Stem Cells Int.* **2016**, 7154327 (2016).
41. M. Minoux, F. M. Rijli, Molecular mechanisms of cranial neural crest cell migration and patterning in craniofacial development. *Development* **137**, 2605–2621 (2010).
42. M. L. Bustos, L. Huleihel, M. G. Kapetanaki, C. L. Lino-Cardenas, L. Mroz, B. M. Ellis, B. J. McVerry, T. J. Richards, N. Kaminski, N. Cerdenes, A. L. Mora, M. Rojas, Aging mesenchymal stem cells fail to protect because of impaired migration and antiinflammatory response. *Am. J. Respir. Crit. Care Med.* **189**, 787–798 (2014).
43. M. La Noce, L. Mele, V. Tirino, F. Paino, A. De Rosa, P. Naddeo, P. Papagerakis, G. Papaccio, V. Desiderio, Neural crest stem cell population in craniomaxillofacial development and tissue repair. *Eur. Cells Mater.* **28**, 348–357 (2014).
44. M. Cáceres, A. Oyarzun, P. C. Smith, Defective wound-healing in aging gingival tissue. *J. Dent. Res.* **93**, 691–697 (2014).
45. C. Florina Andreescu, L. Leila Mihai, M. Răescu, M. Jana Țuculină, C. N. Cumpătă, D. Lucia Ghergic, Age influence on periodontal tissues: A histological study. *Rom. J. Morphol. Embryol.* **54**, 811–815 (2013).
46. P. Sousa-Victor, L. García-Prat, A. L. Serrano, E. Perdiguero, P. Muñoz-Cánoves, Muscle stem cell aging: Regulation and rejuvenation. *Trends Endocrinol. Metab.* **26**, 287–296 (2015).
47. A. Aldahmash, Skeletal stem cells and their contribution to skeletal fragility: Senescence and rejuvenation. *Biogerontology* **17**, 297–304 (2016).
48. H. Lin, J. Sohn, H. Shen, M. T. Langhans, R. S. Tuan, Bone marrow mesenchymal stem cells: Aging and tissue engineering applications to enhance bone healing. *Biomaterials* **203**, 96–110 (2019).
49. S. D. Gopinath, T. A. Rando, Stem cell review series: Aging of the skeletal muscle stem cell niche. *Aging Cell* **7**, 590–598 (2008).
50. Y. Su, C. Chen, L. Guo, J. Du, X. Li, Y. Liu, Ecological balance of oral microbiota is required to maintain oral mesenchymal stem cell homeostasis. *Stem Cells* **36**, 551–561 (2018).
51. G. Hajishengallis, Aging and its impact on innate immunity and inflammation: Implications for periodontitis. *J. Oral Biosci.* **56**, 30–37 (2014).

52. Y. G. Kim, S. M. Lee, S. Bae, T. Park, H. Kim, Y. Jang, K. Moon, H. Kim, K. Lee, J. Park, J. S. Byun, D. Y. Kim, Effect of aging on homeostasis in the soft tissue of the periodontium: A narrative review. *J. Pers. Med.* **11**, 58 (2021).
53. A. P. Beltrami, D. Cesselli, C. A. Beltrami, At the stem of youth and health. *Pharmacol. Ther.* **129**, 3–20 (2011).
54. X. Feng, J. Xing, G. Feng, D. Huang, X. Lu, S. Liu, W. Tan, L. Li, Z. Gu, P16INK4A mediates age-related changes in mesenchymal stem cells derived from human dental pulp through the DNA damage and stress response. *Mech. Ageing Dev.* **141-142**, 46–55 (2014).
55. R. L. Yang, H. M. Huang, C. S. Han, S. J. Cui, Y. K. Zhou, Y. H. Zhou, Serine metabolism controls dental pulp stem cell aging by regulating the dna methylation of p16. *J. Dent. Res.* **100**, 90–97 (2021).
56. A. Azaripour, T. Lagerweij, C. Scharfbillig, A. E. Jadczak, B. Van Der Swaan, M. Molenaar, R. Van Der Waal, K. Kielbassa, W. Tigchelaar, D. I. Picavet, A. Jonker, E. M. L. Hendrikx, V. V. V. Hira, M. Khurshed, C. J. F. V. Noorden, Three-dimensional histochemistry and imaging of human gingiva. *Sci. Rep.* **8**, 1647 (2018).
57. A. Can, H. Coskun, The rationale of using mesenchymal stem cells in patients with COVID-19-related acute respiratory distress syndrome: What to expect. *Stem Cells Transl. Med.* **9**, 1287–1302 (2020).
58. M. A. Avanzini, M. Mura, E. Percivalle, F. Bastaroli, S. Croce, C. Valsecchi, E. Lenta, G. Nykjaer, I. Cassaniti, J. Bagnarino, F. Baldanti, M. Zecca, P. Comoli, M. Gnecchi, Human mesenchymal stromal cells do not express ACE2 and TMPRSS2 and are not permissive to SARS-CoV-2 infection. *Stem Cells Transl. Med.* **10**, 636–642 (2021).
59. G. Matute-Bello, G. Downey, B. B. Moore, S. D. Groshong, M. A. Matthay, A. S. Slutsky, W. M. Kuebler; Acute Lung Injury in Animals Study Group, An official american thoracic society workshop report: Features and measurements of experimental acute lung injury in animals. *Am. J. Respir. Cell Mol. Biol.* **44**, 725–738 (2011).
60. S. S. Batah, A. T. Fabro, Pulmonary pathology of ARDS in COVID-19: A pathological review for clinicians. *Respir. Med.* **176**, 106239 (2021).
61. F. Debacq-Chainiaux, J. D. Erusalimsky, J. Campisi, O. Toussaint, Protocols to detect senescence-associated beta-galactosidase (SA-βgal) activity, a biomarker of senescent cells in culture and in vivo. *Nat. Protoc.* **4**, 1798–1806 (2009).
62. A. Suarez-Arnedo, F. T. Figueroa, C. Clavijo, P. Arbeláez, J. C. Cruz, C. Muñoz-Camargo, An ImageJ plugin for the high throughput image analysis of in vitro scratch wound healing assays. *PLOS ONE* **15**, e0232565 (2020).
63. P. P. C. Souza, P. Lundberg, I. Lundgren, F. A. C. Magalhães, C. M. Costa-Neto, U. H. Lerner, Activation of Toll-like receptor 2 induces B_1 and B_2 kinin receptors in human gingival fibroblasts and in mouse gingiva. *Sci. Rep.* **9**, 2973 (2019).
64. R. Rizzo, G. Lanzoni, M. Stignani, D. Campioni, F. Alviano, F. Ricci, P. L. Tazzari, L. Melchiorri, S. Z. Scalinci, A. Cuneo, L. Bonsi, F. Lanza, G. P. Bagnara, O. R. Baricordi, A simple method for identifying bone marrow mesenchymal stromal cells with a high immunosuppressive potential. *Cytotherapy* **13**, 523–527 (2011).
65. M. C. Herzig, B. A. Christy, R. K. Montgomery, C. P. Delavan, K. J. Jensen, S. E. Lovelace, C. Cantu, C. L. Salgado, A. P. Cap, J. A. Bynum, Interactions of human mesenchymal stromal cells with peripheral blood mononuclear cells in a mitogenic proliferation assay. *J. Immunol. Methods* **492**, 113000 (2021).
66. D. Hartl, S. Krauss-Etschmann, B. Koller, P. L. Hordijk, T. W. Kuijpers, F. Hoffmann, A. Hector, E. Eber, V. Marcos, I. Bittmann, O. Eickelberg, M. Griese, D. Roos, Infiltrated neutrophils acquire novel chemokine receptor expression and chemokine responsiveness in chronic inflammatory lung diseases. *J. Immunol.* **181**, 8053–8067 (2008).

Acknowledgments: We acknowledge the central instrumentation facility, Savitribai Phule Pune University (SPPU), Pune for confocal microscopy and scanning electron microscopy facility. We also thank FACS facility and confocal microscopy facility at the National Centre for Cell Science (NCCS), Pune (Department of Biotechnology, Government of India funded). We extend appreciation to P. Wangikar, PRADO, Pune for providing us the animal facility and the necessary infrastructure for animal experimentation A.J., M.P., and G.B.T. thank Deenanath Mangeshkar Hospital and Research Centre (DMHRC), Pune for the Institutional Ethics Committee approval for human gingival tissue samples. **Funding:** G.B.T. and A.M.D. thank the Department of Science and Technology (DST INSPIRE scheme), Government of India (grant number, IFA13 LSBM73), for the fellowship and the research grant. G.B.T. acknowledges funding from Rashtriya Ucchatar Sikhsha Abhiyaan (RUSA), Government of India and University with Potential for Excellence (UPE-II), SPPU, Pune. G.B.T. also thanks DST (KIRAN-WOSB scheme), Government of India (grant number DST/WOS-B/HN-1/2021) for fellowship and research grant support. J.R.D. thanks Lady Tata Memorial Trust, Tata Trusts, India for the junior and senior research fellowship (JRF and SRF). S.S.C. thanks Bharatratna J.R.D. Tata research fellowship scheme, SPPU, Pune. P.S.P. thanks RUSA for the fellowship. S.B. extends gratitude to the Department of Biotechnology, Government of India for the fellowship (DBT-SRF). S.T.M. thanks UPE-II for the fellowship. **Author contributions:** J.R.D. performed all experiments, collected the data, analyzed the observations, and drafted the manuscript. S.S.C. performed neuronal differentiation, quantified adipogenesis, assisted in animal experiments, and contributed in review of literature. S.B. assisted in animal experiments, flow cytometry, and real-time PCR analysis. K.U.D. carried out experiments for colony formation and estimation of SA-β-gal and assisted in animal experiments. P.M.S. carried out MTT assay and population doubling experiments. N.B.S. performed wound healing experiments. S.T.M. conducted animal experiments. A.M.D. carried out initial cell culture experiments related to collection of gingival tissue samples and isolation of GMSCs. P.S.P. assisted in animal experiments related to ALI. M.P. and A.J. provided gingival tissue samples during their routine clinical procedures. P.A.C. provided useful insights into gingival tissue architecture and assisted in correlating the data to gingival physiology. R.K.S. provided expert comments about the results and data analysis and contributed in compilation of animal experiment data. G.B.T. conceived the project, designed the experiments, analyzed the data, and compiled the manuscript. **Competing interests:** The authors declare that they have no competing interest. **Data and materials availability:** All data needed to evaluate the conclusions in the paper are present in the paper and/or the Supplementary Materials.

Submitted 1 October 2021
Accepted 6 May 2022
Published 24 June 2022
10.1126/sciadv.abm6504